agene). A 1.8-kb Xho I–Bam HI fragment containing most of the Bcl-x coding region was replaced with either a PGK-*neo* polyadenylate [poly(A)] cassette or a PGK-*hyg* poly(A) cassette. The targeting vectors, pXKO-NEO and pXKO-HYG, contain a 6.0-kb region of homology 5′ and 1.0 kb 3′ of the drug-resistance markers and a PGK-*tk* poly(A) cassette. Transfections and selections were performed as described (*3*). DNAs prepared from ES cells were digested with Eco RV, transferred to a nylon membrane, and then hybridized with the 0.4-kb Kpn I–Pst I probe that flanked the 3′ homology region. Expected sizes for wild-type *bcl-x*, mutant *bcl-x* by pXKO-NEO, and mutant *bcl-x* by pXKO-HYG are 9.8, 7.0, and 5.5 kb and were detected in wild-type, *bcl-x*$^{+/-}$, and *bcl-x*$^{-/-}$ ES clones, respectively.
10. R. W. Oppenheim, *Annu. Rev. Neurosci.* **14**, 453 (1991).
11. B. Riederer and A. Matus, *Proc. Natl. Acad. Sci. U.S.A.* **82**, 6006 (1985); R. P. Tucker, L. I. Binder, A. I. Matus, *J. Comp. Neurol.* **271**, 44 (1988).
12. Y. Gavrieli, Y. Sherman, S. A. Ben-Sasson, *J. Cell Biol.* **119**, 493 (1992).
13. A. Jakobovits *et al.*, *Proc. Natl. Acad. Sci. U.S.A.* **90**, 2551 (1993).
14. J. Chen, R. Lansford, V. Stewart, F. Young, F. W. Alt, *ibid.*, p. 4528; J. Chen *et al.*, *Immunity* **1**, 65 (1994).
15. ES-derived thymocytes were purified with an antibody to CD8 (anti-CD8) and magnetic beads from *bcl-x*$^{-/-}$ or wild-type RAG-2 chimeric mice as described (*3*). DNAs prepared from the purified CD8-positive thymocytes were subjected to Southern blot analysis as described above.
16. D. Kitamura *et al.*, *Cell* **69**, 823 (1992).
17. K.-i. Nakayama, K. Nakayama, L. B. Dustin, D. Y. Loh, in preparation.
18. V. L. J. Tybulewicz, C. E. Crawford, P. K. Jackson, R. T. Bronson, R. C. Mulligan, *Cell* **65**, 1153 (1991); P. L. Schwartzberg *et al.*, *ibid.*, p. 1165.
19. E. Y.-H. P. Lee *et al.*, *Nature* **359**, 288 (1992); T. Jacks *et al.*, *ibid.*, p. 295; A. R. Clarke *et al.*, *ibid.*, p. 328.
20. P. J. Welch and J. Y. J. Wang, *Cell* **75**, 779 (1993).
21. D. W. Goodrich, N. P. Wang, Y.-W. Qian, E. Y.-H. P. Lee, W.-H. Lee, *ibid.* **67**, 293 (1991).
22. C. L. Sawyers, J. McLaughlin, A. Goga, M. Havlik, O. Witte, *ibid.* **77**, 121 (1994).
23. One of four *bcl-x*$^{-/-}$ mice at E12.5 and two E13.5 *bcl-x*$^{-/-}$ mice were examined histologically and showed autolytic changes throughout the embryonic tissues indicative of intrauterine death. Careful examination of the three viable E12.5 *bcl-x*$^{-/-}$ embryos showed no obvious gross fetal abnormality, and histologic examination of two E12.5 *bcl-x*$^{-/-}$ placentas showed normal maternal and fetal components. In the embryonic mouse, yolk-sac–derived nucleated red blood cells begin to disappear from the circulation around E12, when the liver becomes the principal source of hematopoietic activity [M. H. Kaufmann, *The Atlas of Mouse Development* (Academic Press, San Diego, CA, 1992), p. 128]. Because the *bcl-x*$^{-/-}$ mice were paler, died at approximately E13, and showed a marked increase in TUNEL-labeled nuclei in the hematopoietic elements of the liver, it is possible that a defect in hepatic hematopoiesis, coupled with declining numbers of yolk sac–derived red cells, produces hypoxic damage to the embryo, resulting in death.
24. Thymocytes and BM and LN cells ($1 \times 10^6$ cells each) were prepared from wild-type and *bcl-x*$^{-/-}$ B6 chimeric mice and were stained with anti-Ly9.1–fluorescein isothiocyanate (FITC), and anti-CD4–phycoerythrin (PE) and anti-CD8–biotin, or anti-B220–PE and anti-immunoglobulin M (IgM)–biotin (PharMingen). For RAG-2 chimeric mice, cells were stained with anti-CD8–FITC and anti-CD4–PE, or anti-IgM–FITC or anti-IgD–FITC (Southern Biotechnology) and anti-B220–PE. Biotin conjugate was revealed by RED 613-streptavidin (Gibco BRL). Dead cells were excluded by staining with propidium iodide (Boehringer Mannheim). Flow cytometric analysis was done on FACScan computer and software (Becton Dickinson).
25. Whole embryos were fixed in 4% paraformaldehyde and embedded in paraffin, and 5-μm-thick sagittal sections were cut at multiple levels. Sections were alternatively stained with hematoxylin-eosin and with cresyl violet. Unstained sections were processed for immunostaining as described [M. L. Hermiston, C. B. Latham, J. I. Gordon, K. A. Roth, *J. Histochem. Cytochem.* **40**, 1283 (1992)]. A mouse monoclonal antibody to MAP2 (Sigma) was used at a dilution of 1:1000 to detect differentiating neurons. Primary antibodies were detected with a CY-3-conjugated donkey antiserum to mouse IgG (Jackson Immunoresearch Laboratories). Omission of the primary antibody resulted in only weak, nonspecific labeling of the blood vessels. After immunolabeling, sections were incubated for 10 min at room temperature in bisbenzamide (0.04 μg/ml) (Hoechst 33258, Sigma) to label cell nuclei. Slides were viewed and photographed with a Zeiss Axioskop fluorescence microscope.
26. Apoptotic cells were identified by the TUNEL method (*12*) modified to detect incorporated digoxygenin-dUTP with either alkaline phosphatase or gold-conjugated sheep antibody to digoxygenin.
27. In situ hybridizations were performed as described [H. Sawa, B. E. Sobel, S. Fujii, *Circ. Res.* **73**, 671 (1993)]. For construction of RNA probes, pBluescript SKII+ plasmid containing a 0.8-kb mouse *bcl-x* complementary DNA insert was linearized by restriction digestion with Xho I or Not I (for antisense and sense, respectively) and transcribed with T7 or T3 RNA polymerase in the presence of $^{35}$S-labeled uridine triphosphate (UTP).
28. We thank F. W. Alt for RAG-2–deficient mice, P. Mombaerts for E14 ES cell line, J. Y. J. Wang for helpful suggestions, and L. B. Dustin and I. T. Chan for critical reading of the manuscript. Supported by the Howard Hughes Medical Institute (D.Y.L.) and the Japan Society for the Promotion of Science (N.M.).

2 November 1994; accepted 9 February 1995

# Synaptic Desensitization of NMDA Receptors by Calcineurin

Gang Tong,* Dawn Shepherd, Craig E. Jahr†

**Desensitization is a phenomenon that is common to many ligand-gated ion channels but has been demonstrated only rarely with physiological stimulation. Numerous studies describe desensitization of the *N*-methyl-D-aspartate (NMDA) subtype of glutamate receptor by exogenous agonists, but whether synaptic stimulation causes desensitization has been unknown. Synaptic stimulation of NMDA receptors on rat hippocampal neurons resulted in desensitization that was prevented by intracellular 1,2-bis(*o*-aminophenoxy)ethane-*N*,*N*,*N*′,*N*′-tetraacetic acid (BAPTA), adenosine-5′-*O*-(3-thiotriphosphate) (ATP-γ-S), or inhibitors of phosphatase 2B (calcineurin), but not by inhibitors of phosphatases 1 and 2A or of tyrosine phosphatases. Synaptic NMDA receptors may fluctuate between phosphorylated and dephosphorylated forms, depending on the rate of synaptic stimulation and the magnitude of the associated influx of calcium through NMDA receptors.**

The magnitude of $Ca^{2+}$ influx through synaptically activated NMDA receptor channels not only affects the amplitude and lifetime of long-term synaptic plasticity at certain central synapses, but also is a factor in whether subsequent synaptic strength is increased or decreased (*1–3*). Several species of protein phosphatases cause diminished NMDA channel activity (*4–6*), which may result in decreased $Ca^{2+}$ influx during synaptic stimulation. In addition, calcineurin activity stimulated by brief elevations of intracellular $Ca^{2+}$ concentration (*7*) causes the development of a glycine-insensitive form (*8, 9*) of NMDA receptor desensitization. Because NMDA receptor channels are very permeable to $Ca^{2+}$ (*10*), synaptic activation may enable this form of desensitization and may result in a negative feedback of NMDA receptor synaptic activation. If desensitization is enhanced by synaptic stimulation, the decrease in ion flux will result in smaller intracellular $Ca^{2+}$ transients that could shift the balance between long-term potentiation (LTP) and long-term depression (LTD) of synaptic strength (*1–3*).

Isolated cultured rat hippocampal neurons make synapses onto themselves (*11*) and were used to measure NMDA receptor desensitization induced by synaptic stimulation. The synapses were conditioned by stimulating them four times within 75 ms (*12*) and were tested with a single stimulus after a variable interval (0.8 to 7.5 s). The depression of the test excitatory postsynaptic current (EPSC) relative to the first conditioning EPSC could result from a combination of a lower presynaptic release probability (synaptic depression or presynaptic inhibition) and a decreased sensitivity of postsynaptic receptors (desensitization). The amount of depression resulting from NMDA receptor desensitization was estimated by comparing the amplitudes of test EPSCs conditioned by the four-pulse conditioning stimulus delivered in the presence or absence of the competitive antagonist of the NMDA receptor, D-2-amino-5-phosphonopentanoic acid (D-AP5, 100 μM) (Fig. 1A). In the presence of D-AP5, glutamate released by

G. Tong and C. E. Jahr, Vollum Institute and Department of Cell Biology and Anatomy, Oregon Health Sciences University, Portland, OR 97201–3098, USA.
D. Shepherd, Vollum Institute, Oregon Health Sciences University, Portland, OR 97201–3098, USA.

*Present address: Department of Pharmacology, University of California, San Francisco, CA 94143, USA.
†To whom correspondence should be addressed.

conditioning stimuli will not bind to NMDA receptors, and thus agonist-induced desensitization will not occur. We rapidly removed D-AP5 from the synapse by switching to a solution without D-AP5 after the last conditioning stimulus (*13*). Because the probability of release from individual release sites is about 0.5 or lower (*14*), four conditioning stimuli were used to maximize the percentage of release sites (and thus NMDA receptors) that were activated. In saturating concentrations of glycine (20 μM), the test EPSC evoked 1.5 s after delivery of the conditioning stimuli was 78.7 ± 2.0% of the test EPSC evoked after the conditioning stimuli that were applied while D-AP5 was present. This observation indicates that synaptic activation of NMDA receptors results in receptor desensitization that is glycine-insensitive.

These experiments were repeated in an extracellular solution containing 1 mM $Mg^{2+}$ because, at this physiological concentration, $Mg^{2+}$ blocks more than 95% of the NMDA receptor current (and thus $Ca^{2+}$ influx) at a holding potential of −70 mV and about 80% of the current at −40 mV (*15*). When the membrane potential was held at −40 mV for 100 ms after delivery of the conditioning stimuli to approximate normal synaptic transmission, the test EPSC evoked 1.5 s after delivery of the conditioning stimuli was 84.4 ± 3.2% of the test EPSC evoked after the conditioning stimuli that were applied while D-AP5 was present (paired *t* test, $P < 0.005$, $n = 5$) (Fig. 1B). Therefore, the amount of calcium influx in physiological conditions is sufficient to densensitize NMDA receptors. However, when the membrane potential was held at −70 mV continuously, the test EPSCs in the presence and absence of D-AP5 were indistinguishable (100.8 ± 3.0%, $n = 8$). Therefore, partial relief of $Mg^{2+}$ inhibition of NMDA channels is necessary for synaptic activation of NMDA receptor desensitization.

The time course of recovery from desensitization (Fig. 1C) was very similar to that in outside-out patches (*8*, *9*); complete recovery required more than 7.5 s. Periods between conditioning and test EPSCs shorter than 0.8 s were not tested because of the slow decay of synaptic current evoked by the conditioning stimuli, which interfered with the measurement of desensitization, and because of the finite time required to completely wash away D-AP5. Because desensitization in outside-out patches is greatest at much shorter intervals (*8*, *9*), it is likely that shortly after the conditioning stimuli were applied, desensitization was more profound than it was 0.8 s later.

We also monitored (S)-α-amino-3-hydroxy-5-methyl-4-isoxazolepropionic acid (AMPA) receptor EPSCs to control for possible effects of NMDA receptor stimulation on presynaptic release probability—for example, through the action of retrograde transmitters (*3*). Conditioning stimuli were applied in the presence and absence of D-AP5, as described above, but in the absence of AMPA receptor blockers. The test stimulus was given in the presence of D-AP5 so

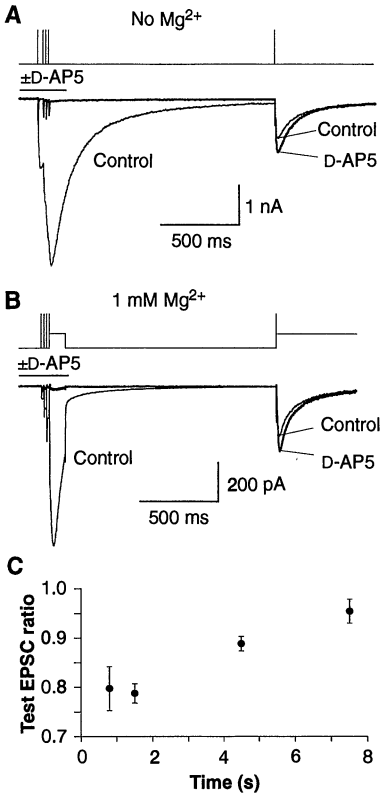


**Fig. 1.** Glycine-insensitive synaptic desensitization of NMDA receptors. (**A**) In the absence of extracellular $Mg^{2+}$, four conditioning NMDA receptor EPSCs were evoked in rapid succession (*12*) in the presence (thick line) or absence (control; thin line) of 100 μM D-AP5; a test EPSC was evoked 1.5 s later (more than 1 s after switching to a solution without D-AP5). The top trace indicates the voltage command protocol used to stimulate the synapse. The holding potential was −70 mV. (**B**) Similar protocol to that used in (A), but in the continuous presence of 1 mM extracellular $Mg^{2+}$ and with voltage jumps to −40 mV (as shown in the upper trace) to allow partial relief of inhibition of NMDA channels during conditioning and test EPSCs. Responses recorded in the continuous presence of D-AP5 were subtracted to remove voltage jump leak currents. (**C**) The time course of recovery from desensitization is plotted as the ratio of the test EPSCs evoked following conditioning stimuli that were delivered in the absence and presence of D-AP5, respectively. EPSC amplitudes were measured from the base line value before delivery of the conditioning stimuli and thus underestimate the degree of desensitization. The two sets of responses were interleaved in time to control for time-dependent changes in synaptic strength.

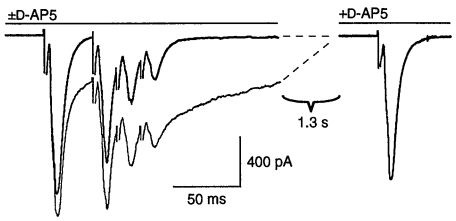


**Fig. 2.** Activation of NMDA receptors does not alter presynaptic release. The same stimulation protocol as in Fig. 1A was used in the absence of AMPA receptor blockers. Test EPSCs are superimposed. The interval between the first conditioning stimulus and the test stimulus was 1.5 s; the gap in records is 1.3 s.

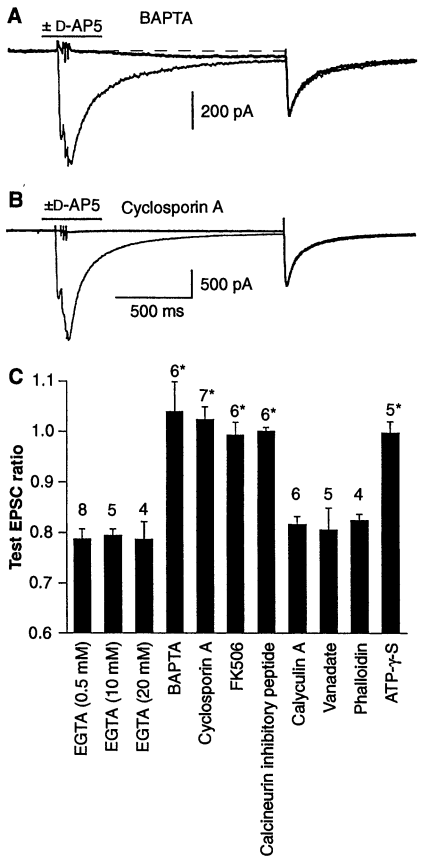


**Fig. 3.** Synaptic desensitization is prevented by internal BAPTA and calcineurin inhibitors. (**A**) The same protocol as that used in Fig. 1A, with an intracellular solution containing 20 mM BAPTA instead of EGTA. The small current that developed after washout of D-AP5 (dotted line is base line) was seen in 37 of 85 recordings and was caused, at least in part, by an increased frequency of spontaneous EPSCs (*23*). (**B**) EPSCs recorded with 200 nM cyclosporin A in external and internal solutions. (**C**) Graph of the ratio of the amplitudes of test EPSCs recorded after conditioning stimuli were applied in the absence or presence of D-AP5. The interval between the first conditioning stimulus and the test stimulus was 1.5 s. The number of cells in each category is printed above the bars. Asterisks indicate significant differences ($P < 0.01$) from the 0.5 mM EGTA condition (analysis of variance). Error bars represent SEM.

that the AMPA receptor EPSC could be recorded in isolation (Fig. 2). Activation of NMDA receptors by the conditioning stimuli had no effect on the amplitude of the AMPA receptor test EPSC (100.1 ± 1.6%, $n$ = 6). AMPA receptor EPSCs recorded in the presence of 2 mM extracellular $Mg^{2+}$ to block NMDA receptor currents were not affected by 100 μM D-AP5 ($n$ = 4).

In outside-out patches, the fast phase of development of glycine-insensitive desensitization is blocked by internal BAPTA, by ATP-γ-S, and by inhibitors of calcineurin (*7*). We used the same manipulations to block the synaptic form of desensitization. Although there was no difference in the amount of desensitization in recordings with 0.5 to 20 mM internal EGTA, 20 mM internal BAPTA blocked desensitization (Fig. 3, A and C). Addition of the specific inhibitors of calcineurin, cyclosporin A (200 to 500 nM), FK506 (200 to 500 nM), or calcineurin inhibitory peptide (270 μM) (*16*), blocked synaptic desensitization after 4 to 7 min of recording (Fig. 3, B and C). Synaptic desensitization was not prevented by calyculin A (200 nM), a phosphatase 1 and 2A inhibitor (*17*); by intracellular vanadate (1 mM), a tyrosine phosphatase inhibitor (*18*); or by phalloidin (1 μM), which stabilizes filamentous actin (*19*) and has been shown to prevent $Ca^{2+}$-dependent rundown of the NMDA receptor (*20*) (Fig. 3C). However, inclusion of 1 mM ATP-γ-S in the internal solution blocked desensitization within 4 to 6 min of the start of recordings (Fig. 3C).

These results indicate that the phosphorylation state of the NMDA receptor, or of an associated protein, alters NMDA receptor desensitization. Because synaptic desensitization is dependent on $Ca^{2+}$ influx through NMDA receptor channels and subsequent activation of calcineurin, synaptic NMDA receptor complex may be dephosphorylated with each quantum of released transmitter. Inhibition of the effect of $Ca^{2+}$ influx by chelation required the extremely fast binding properties of BAPTA (*21*); EGTA at concentrations that result in smaller amounts of free $Ca^{2+}$ at equilibrium did not block synaptic desensitization. This observation suggests that the site of action of $Ca^{2+}$ is very close to the cytoplasmic face of synaptic NMDA receptor channels. Calcineurin is reported to be associated with postsynaptic densities (*22*); this provides the spatial specificity for this mechanism.

Because recovery from desensitization requires several seconds, regulation of NMDA receptor function by this mechanism may be strong enough to significantly alter $Ca^{2+}$-dependent processes invoked by repetitive synaptic activity. The balance between homosynaptic LTD and LTP in the hippocampus depends in part on the magnitude of the increase of intracellular $Ca^{2+}$ concentration as a result of influx through NMDA channels (*1–3*). Low-frequency stimulation (1 Hz) increases the intracellular $Ca^{2+}$ concentration sufficiently to induce a calcineurin-dependent homosynaptic LTD (*2*), whereas high-frequency stimulation (100 Hz) raises $Ca^{2+}$ to concentrations at which other $Ca^{2+}$-dependent reactions predominate and produce LTP (*3*). Thus, inhibition of induction of LTD by calcineurin blockers (*2*) may in part be a result of decreased NMDA receptor desensitization leading to greater intracellular $Ca^{2+}$ concentrations during low-frequency stimulation.

## REFERENCES AND NOTES


1. S. M. Dudek and M. F. Bear, *Proc. Natl. Acad. Sci. U.S.A.* **89**, 4363 (1992).
2. R. M. Mulkey *et al.*, *Nature* **369**, 486 (1994).
3. M. F. Bear and R. C. Malenka, *Curr. Opin. Neurobiol.* **4**, 389 (1994).
4. L.-Y. Wang *et al.*, *Nature* **369**, 230 (1994).
5. D. N. Lieberman and I. Mody, *ibid.*, p. 235.
6. Y. T. Wang and M. W. Salter, *ibid.*, p. 233.
7. G. Tong and C. E. Jahr, *J. Neurophysiol.* **72**, 754 (1994).
8. W. Sather *et al.*, *Neuron* **4**, 725 (1990); I. V. Chizhmakov *et al.*, *J. Physiol. (London)* **448**, 453 (1992).
9. R. A. J. Lester and C. E. Jahr, *J. Neurosci.* **12**, 635 (1992).
10. M. L. Mayer *et al.*, *ibid.* **7**, 3230 (1987); P. Ascher and L. Nowak, *J. Physiol. (London)* **399**, 247 (1988); C. E. Jahr and C. F. Stevens, *Nature* **325**, 522 (1987); C. Rosenmund *et al.*, *J. Neurophysiol.* **73**, 427 (1995).
11. J. M. Bekkers and C. F. Stevens, *Proc. Natl. Acad. Sci. U.S.A.* **88**, 7834 (1991). Whole-cell recordings of autaptic currents and miniature EPSCs were made (Axopatch-1D) with low-resistance patch pipettes (0.5 to 2.5 megohms) containing 150 mM potassium gluconate, 10 mM NaCl, 10 mM Hepes, 0.5 mM EGTA (except where noted), 4 mM magnesium adenosine triphosphate, and 0.2 mM guanosine triphosphate, adjusted to pH 7.3 with KOH. Control extracellular solution contained 160 mM NaCl, 3 mM KCl, 5 mM Hepes, 2 mM $CaCl_2$, 20 μM glycine, 5 μM 2,3-dihydroxy-6-nitro-7-sulfamoyl-benzo(F)quinoxaline (NBQX), and 50 to 100 μM picrotoxin, adjusted to pH 7.4 with NaOH. Autaptic EPSCs were evoked with voltage jumps to −20 or 0 mV from a holding potential of −60 to −90 mV (durations of 0.3 to 2 ms). Currents were sent through a low-pass filter at 0.5 to 10 kHz and were digitally sampled at 1 to 50 kHz. Series resistance compensation (80 to 100%) was used in all experiments. All experiments were performed at 22° to 24°C. Data are expressed as mean ± SEM.
12. The first two stimuli of the conditioning train were delivered 35 ms apart to allow for accurate measurement of the amplitude of the first EPSC. The second to fourth stimuli were delivered 20 ms apart.
13. Solution changes were made with gravity-fed flow tubes (*7*, *9*).
14. N. A. Hessler *et al.*, *Nature* **366**, 569 (1993); C. Rosenmund *et al.*, *Science* **262**, 754 (1993).
15. C. E. Jahr and C. F. Stevens, *J. Neurosci.* **10**, 3178 (1990).
16. J. Kunz and N. N. Hall, *Trends Biochem. Sci.* **18**, 334 (1993); Y. Hashimoto, B. A. Perrino, T. R. Soderling, *J. Biol. Chem.* **265**, 1924 (1990). FK506 was added to the external solution, calcineurin inhibitory peptide was added to the internal solution, and cyclosporin A was added to both solutions.
17. H. Ishihara *et al.*, *Biochem. Biophys. Res. Commun.* **159**, 871 (1989). Calyculin A was added to the external solution.
18. G. Swarup *et al.*, *ibid.* **107**, 1104 (1982).
19. J. A. Cooper, *J. Cell Biol.* **105**, 1473 (1987).
20. C. Rosenmund and G. L. Westbrook, *Neuron* **10**, 805 (1993).
21. R. Pethig *et al.*, *Cell Calcium* **10**, 491 (1989).
22. S. Goto *et al.*, *Brain Res.* **397**, 161 (1986).
23. In two cells that exhibited the development of this current after washout of D-AP5, the frequencies of AMPA receptor spontaneous EPSCs (in the presence of D-AP5 and 2 mM $Mg^{2+}$) recorded after the four-pulse conditioning stimulus was delivered were two and four times, respectively, the unstimulated frequency. In an additional cell, the frequency increased to a point where spontaneous events summated and could not be counted. It is unlikely that free glutamate remained in the cleft after delivery of the conditioning stimulus because the D-AP5 was washed out in this interval; this result suggests that the synaptic clefts were well perfused.


24. Supported by NIH grant NS21419.

29 August 1994; accepted 21 December 1994


# Storage of 7 ± 2 Short-Term Memories in Oscillatory Subcycles


John E. Lisman* and Marco A. P. Idiart



**Psychophysical measurements indicate that human subjects can store approximately seven short-term memories. Physiological studies suggest that short-term memories are stored by patterns of neuronal activity. Here it is shown that activity patterns associated with multiple memories can be stored in a single neural network that exhibits nested oscillations similar to those recorded from the brain. Each memory is stored in a different high-frequency ("40 hertz") subcycle of a low-frequency oscillation. Memory patterns repeat on each low-frequency (5 to 12 hertz) oscillation, a repetition that relies on activity-dependent changes in membrane excitability rather than reverberatory circuits. This work suggests that brain oscillations are a timing mechanism for controlling the serial processing of short-term memories.**


Some forms of short-term memory appear to be stored by neurons that continue to fire after they are excited by a brief input (*1*). Hebb and others (*2*) proposed that such firing is sustained by reverberation of electrical activity in neuronal loops. We now demonstrate the feasibility of an alternative mechanism that is based on known properties of hippocampal and cortical neurons: Firing is sustained by an increase in mem-